PHASE 1
FINAL REPORT

Central State University
Wilberforce, Ohio 45384

Period: September 1993 - April 1995
Contract: SUB GRANT **NASA # NCC3-326**

Title: Automated Target Acquisition, Recognition and Tracking (ATTRACT)

Principal Investigator: **Mahmoud A. Abdallah, Ph.D., PE.**
Phone : (513) 376-6196
Fax: (513) 376-6679

Date Prepared: December 6, 1995

1- SUMMARY

The primary objective of phase 1 of this research project is to conduct multidisciplinary research that will contribute to fundamental scientific knowledge in several of the USAF critical technology areas. Specifically, neural networks, signal processing techniques, and electro-optic capabilities are utilized to solve problems associated with automated target acquisition, recognition, and tracking. To accomplish the stated objective, several tasks have been identified and were executed.

2- ACCOMPLISHMENTS

This report presents our research efforts at solving the ATTRACT problem using electro-optic systems, neural networks, and image processing techniques. In the electro-optic area, three different algorithms: (a) Fourier-Mellin transform (FMT) based hybrid electro-optic algorithm; (b) joint Fourier transform (JFT) based algorithm; and (c) amplitude-modulated phase only filter (AMPOF) based correlation algorithm are utilized. Using the silhouette of aircraft targets, features were defined and extracted to train a neural network that proved to be very effective in recognizing targets regardless of their orientation and scale. Also, by developing an autoregressive model to recognize aircraft silhouettes, another effective scheme for target recognition was developed.

For the electro-optic systems, our intent is to identify, analyze, and characterize hybrid electro-optic systems which are capable of meeting ATTRACT objectives and whose speed operation is faster than the purely electronic ones. Each of these algorithms are implementable using optical

systems and, therefore, in each the corresponding two-dimensional processing is accomplished in parallel.

2.a. *FMT Based Correlation:* While the classical Vander-Lugt type of correlation [1,2] can be used to handle the ATTRACT problem by employing multiplexed matched filters, it still remains very sensitive to both scale and rotation. Fortunately, one can use a Mellin transform based Vander-Lugt correlator [3,4] for adequately dealing with the issues both rotation and scale. However, such a process will still need the fabrication of a filter or a bank of filters thus slowing down the corresponding computation time. On the other hand, JFT correlation [1,5] has been shown to be capable of real-time matching and tracking operations as it does not involve any filter fabrication. This ongoing FMT effort, accordingly, combines the best of both solutions by cultivating a JFT implementation of Merlin transform based correlation.

Figure 1 shows the system that can implement a traditional JFT correlation. In it the target scene (which may or may not contain a target) as well as the reference scene (target model) are both loaded in a modified liquid crystal television (LCTV) [11,6]. The joint scenes are then Fourier transformed (in parallel) using a Fourier lens and then detected by a CCD camera. The CCD camera information, which corresponds to the square of the joint Fourier transform), is now fed to a second LCTV. The following Fourier lens next performs an inverse Fourier transform information and accordingly the video-processed output corresponds to the correlation of the two scenes. The correlation energy obtained thereby thereafter serves as a measure of correlation.

The Merlin-transform based technique involves the following steps. First, the target scene is Fourier transformed, preferably, by optics. Second, its magnitude is taken through a polar coordinate transformation whereby the rotational shifts about the origin of the rectangular spatial frequency domain is converted into linear shifts. Third, the radial axis of the polar domain is logarithmically scaled which converts scale changes in the Fourier transform space into linear shifts along the radial axis. Figure 2 shows the block diagram describing the implementation of this algorithm. Figure 3 on the other hand shows the system operations obtained by combining the best of two processes - Mellin based algorithm and the real-time JFT architecture. Advantages of this system are as follows. The transformation of the target scene and the reference scene is accomplished in one step and in parallel using only one filter. The phase information is not lost thus maintaining the position information of the targets. Figure 4 shows the corresponding hybrid electro-optical implementation. Figure 5 shows a test result of two square shaped targets but with different scale and rotation. Figure 5(b) includes the logarithmic-polar transformation while Figure 5(c) and 5(d) corresponds to the binarized and edge-enhanced logarithmic-polar transformation. Finally Figure 5(e) shows the degree of correlation between these two scaled and rotated targets.

In this particular area of research, the investigators have accomplished the following objectives:

- Tested a possible Fourier-Mellin joint transform correlator,
- Tested the workability of a hybrid electro-optic joint Fourier transform correlator that uses liquid crystal televisions (LCTVs) for recording the joint scene (i.e., input and

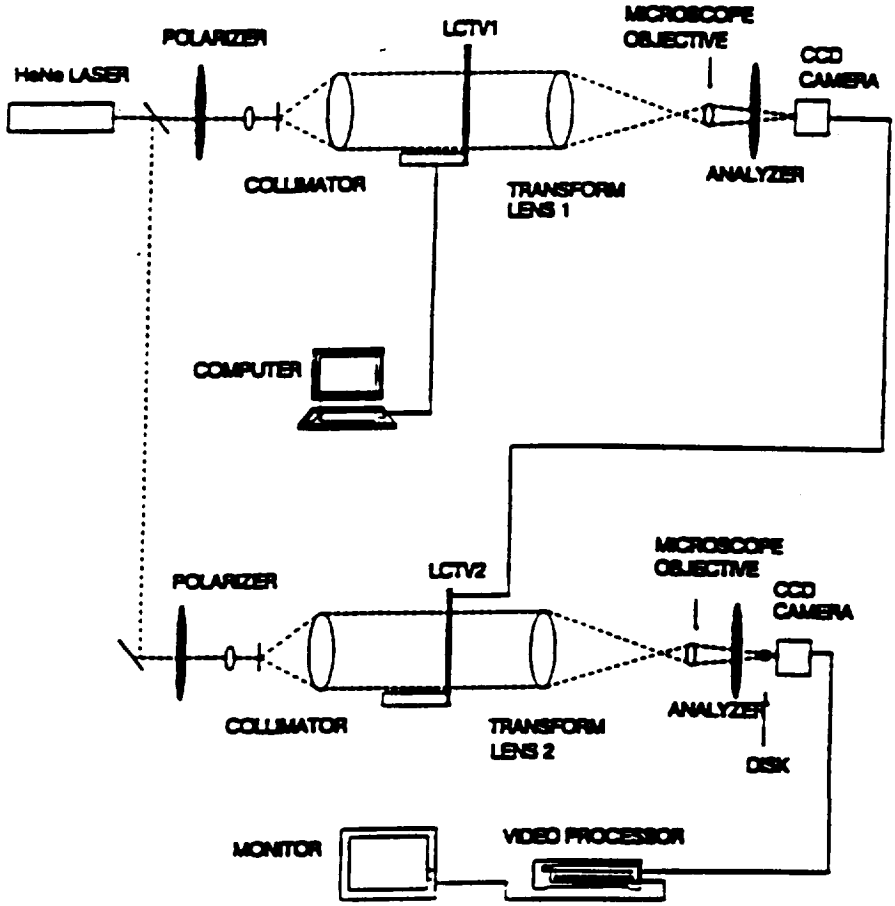

Figure 1, Traditional JFT Correlator

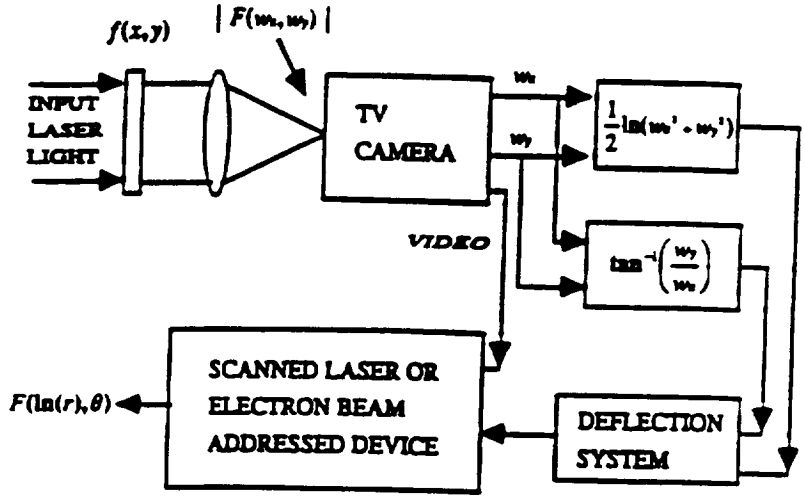

Figure 2, Algorithm Implementation

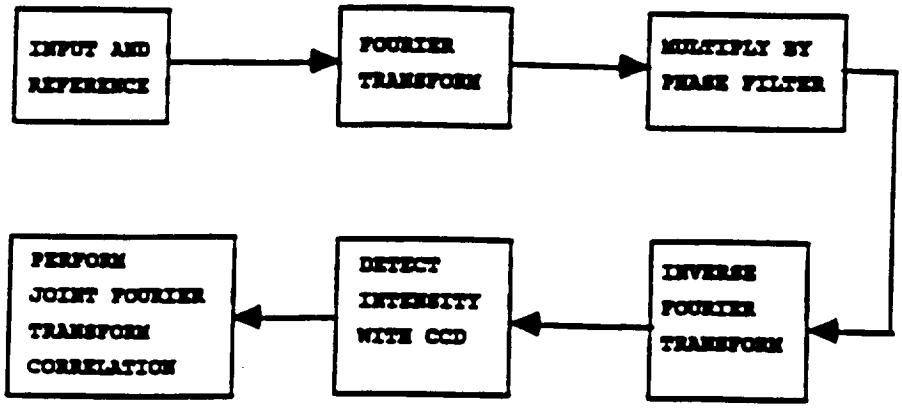

Figure 3, System Operations

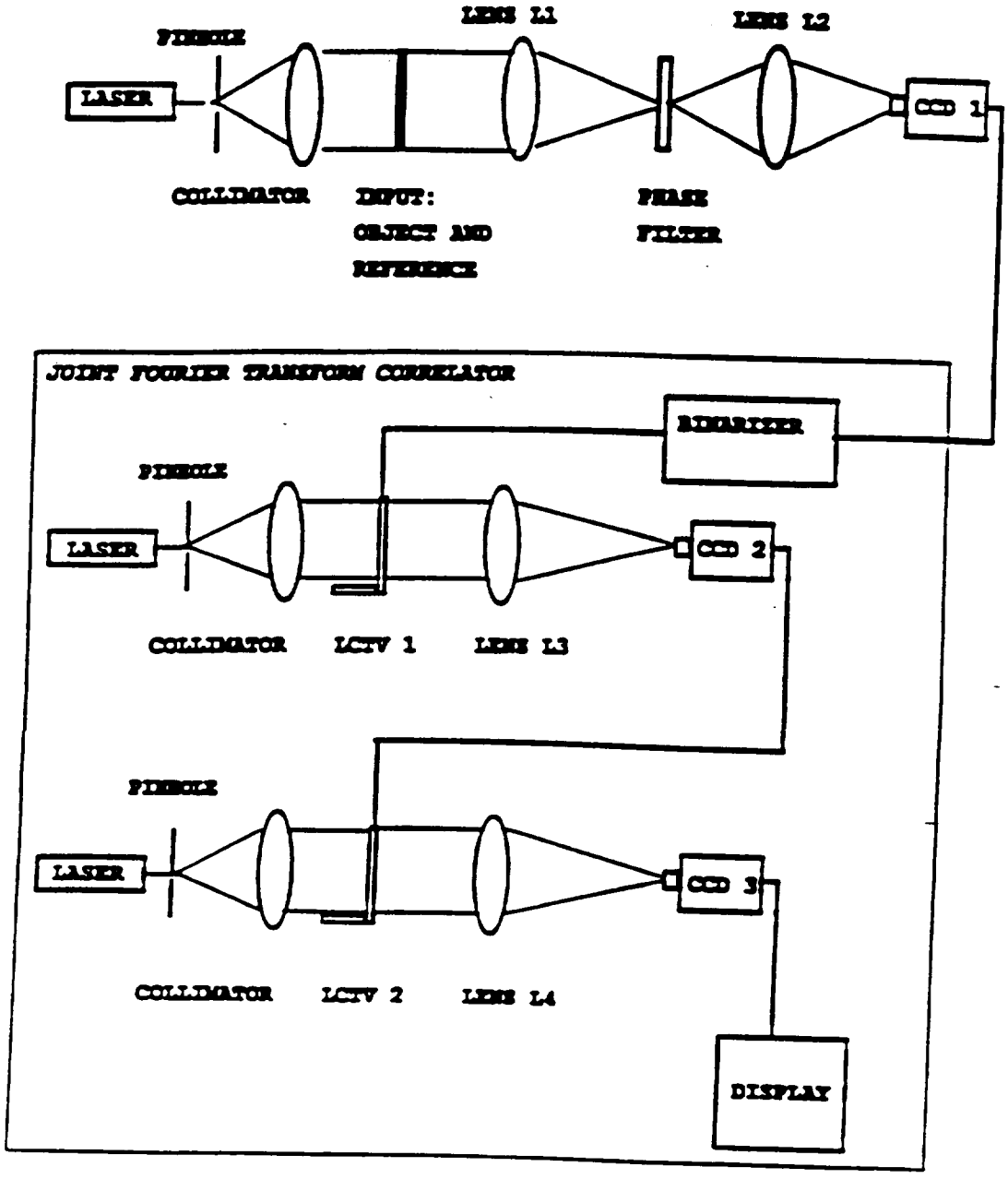

Figure 4, Hybrid Electro-Optical Implementation

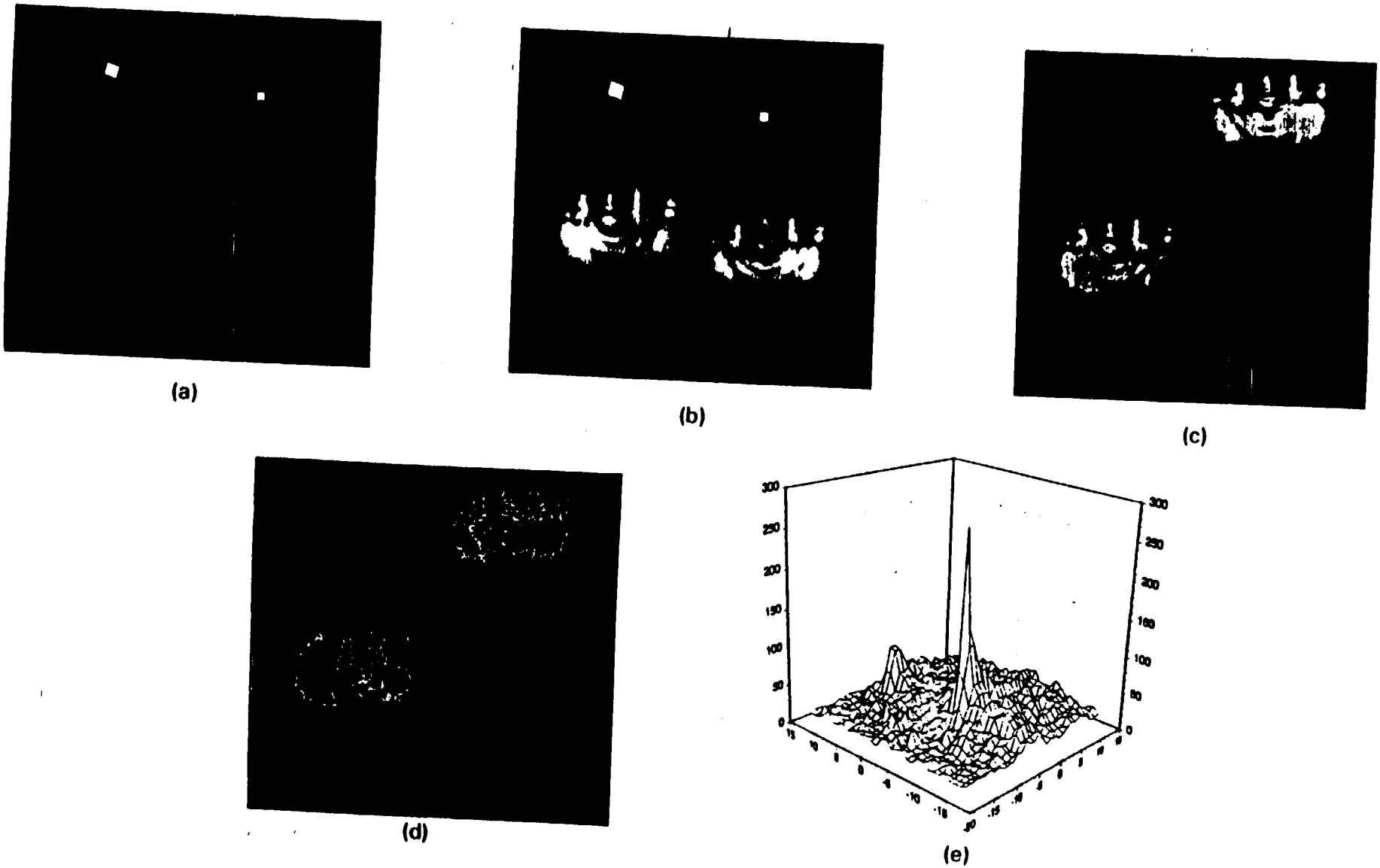

Figure 5, Test Result for Two Square Shaped Targets

reference) and for recording the square of the Fourier transform of the joint scene. Upon taking the Inverse Fourier transform of the square of the joint Fourier transform, we obtain meaningful correlation peaks that can both detect and track the target.

2.b. ***JFT Correlation:*** In practice, in a JFT correlator system, the joint power spectrum (JPS) is binarized based on a hard-clipping non linearity at the Fourier plane to only two values, +1 and -1, before applying the inverse Fourier transform operation on it. While processing target scene that includes multiple targets, the binarization of JPS introduces harmonic correlation peaks that may in turn result in false alarms. This rather serious problem of false alarm is being dealt with in our ongoing ATTRACT work by making use of a fringe-adjusted filter (FAF) [7,8] in the JFT correlator and by modifying the JPS content of it. In this scheme, the JPS is multiplied by the FAF. The FAF H(u,v) is given by B(u,v)/[A(u,v) + |R(u,v)|^2] where A(u,v) and R(u,v) are either constants or functions of u and v and |R(u,v)| is the amplitude of the reference Fourier transform. When multiple targets are present in the scene, then in addition to the autocorrelation between the reference and the targets, additional correlation peaks will be produced because of autocorrelation between the targets themselves. These false alarms are avoided by eliminating the cross-correlation energies between the different targets. This is achieved by displaying the target scene at the JTC input plane without the presence of the reference scene and then recording the target-only power spectrum. With this power spectrum subtracted from JPS, the modified JPS is next processed for the subsequent two operations: multiplication with FAF and an inverse Fourier transformation. The resulting correlation output is expected to be unaffected by any false alarms.

Figure 6 shows the FAF based JFT correlator system. Figure 7a shows a test reference while Figure 7b shows a set of targets in the scene. Figure 8 shows the correlation output at the exact location of the targets and no false alarms.

In JFT related work, the investigators have accomplished the following objectives:

- Designed and tested the JFT correlator far single-target recognition both in the absence of noise and also in the presence of noise.
- To overcome the false alarms, designed the fringe-adjusted filter for JFT applications.
- Tested the JFT correlator for recognizing targets from amongst multiple targets in presence of noise and clutter and under varying illumination conditions.

2.c. ***AMPOF Based Correlation:*** One of the reasons for not often preferring to use a Vander-Lugt type of a matched filter configuration for correlation is that the resulting correlation peak is neither too narrow nor too high during a match [1]. This problem has partly been overcome by devising a phase-only filter [1,9]. However, we have in the past demonstrated an amplitude-modulated phase-only filter [10,11] which has the possibility of providing a yet-larger correlation discrimination as well. As part of the ongoing ATTRACT effort, we are now studying the extent to which this AMPOF amplitude and phase can be descretized. The

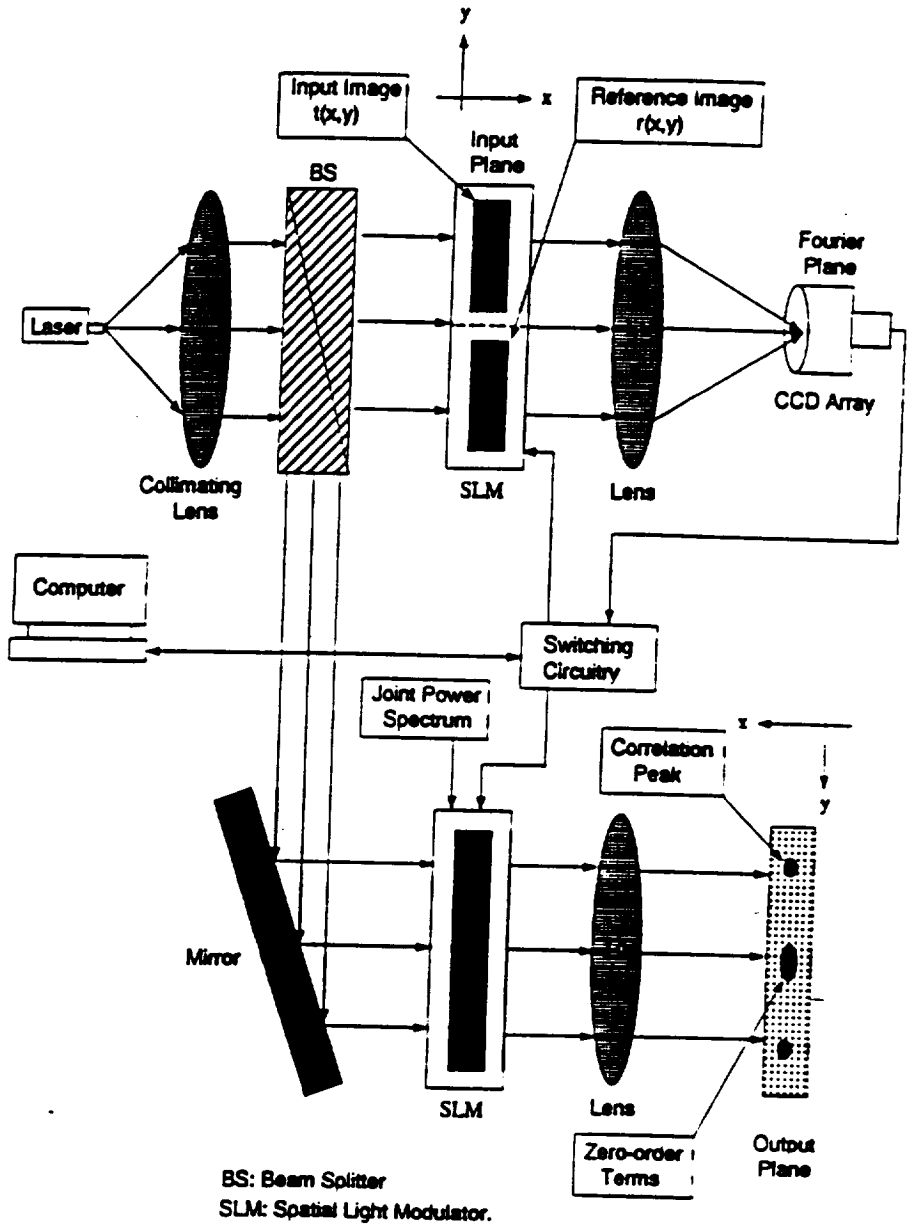

Figure 6, FAF Based JFT Correlator

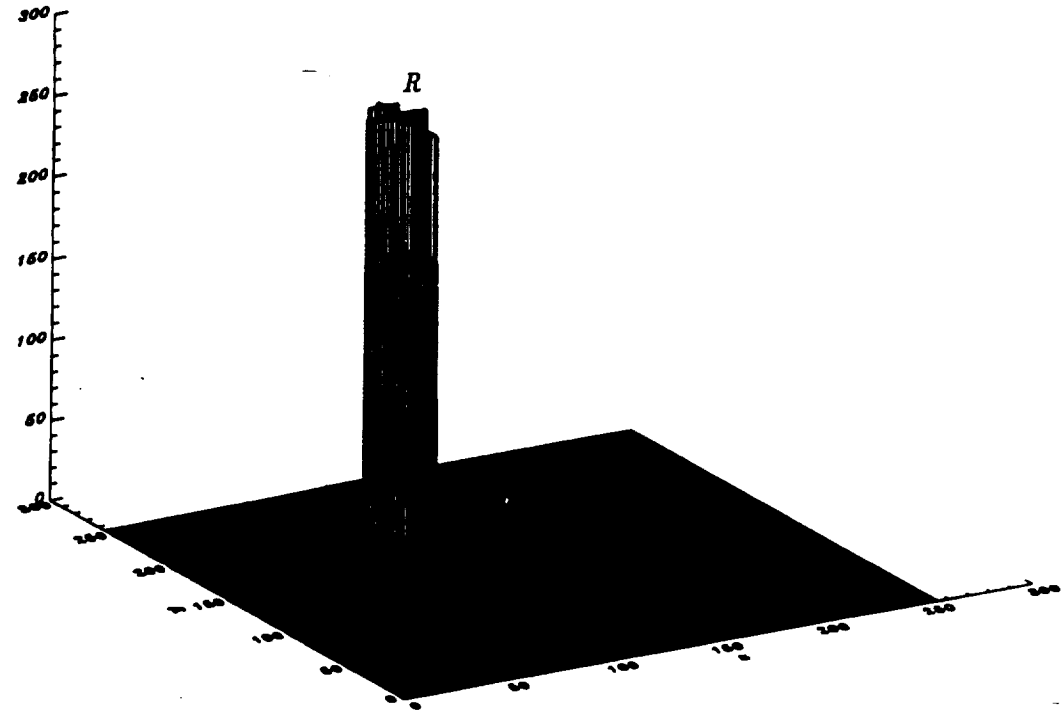

(a)

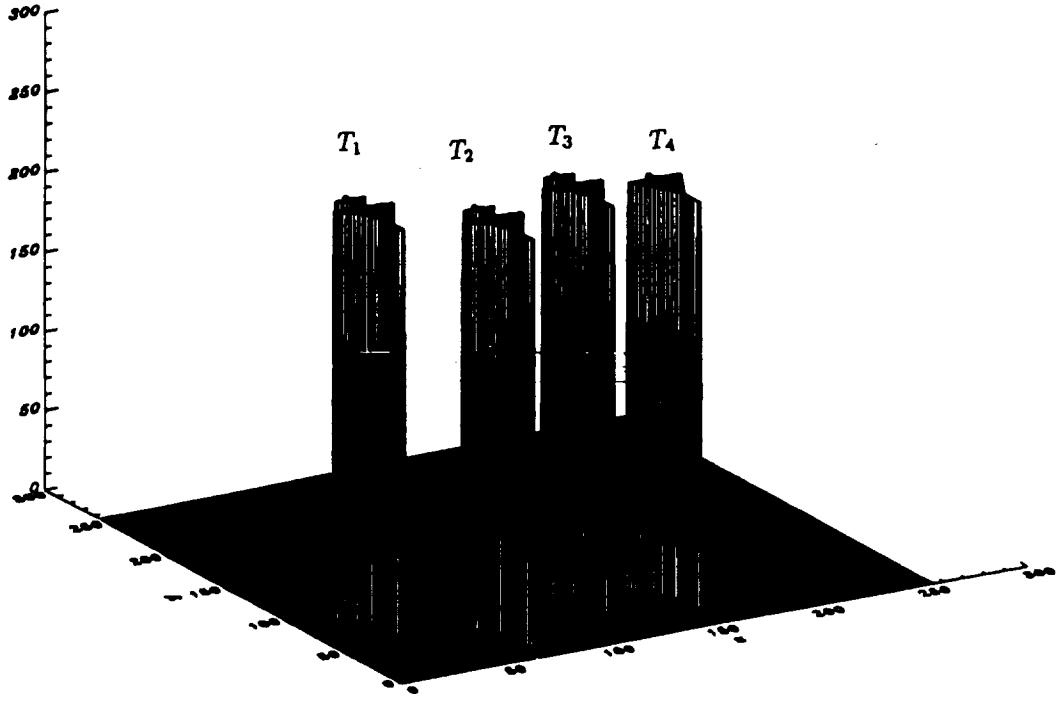

(b)

Figure 7, Reference and Targets Results

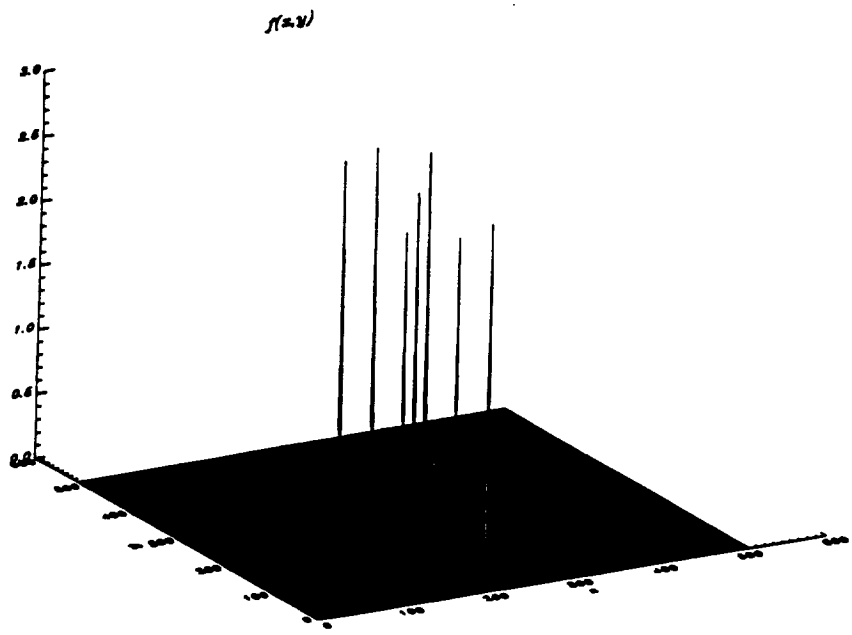

(a)

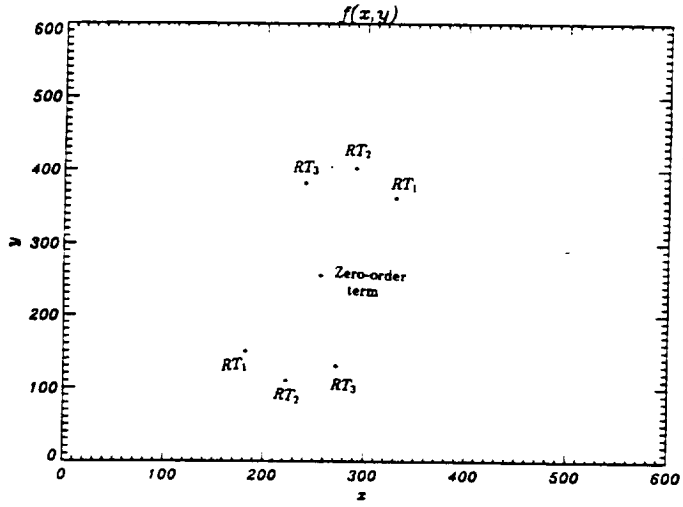

(b)

Figure 8, Correlation Output

discretization of the AMPOF will guarantee its implementation using spatial light modulators thus making the overall correlation system suitable for autonomous and real-time operations.

In AMPOF based architecture, the target scene is Fourier transformed first, then multiplied with the AMPOF function at the Fourier plane, and finally inverse Fourier transformed. The AMPOF function F(u,v) is given by B(u,v) exp[-j p(u,v)]/[|R(u,v)| + A(u,v)] where p(u,v) is the phase component of the reference Fourier transform R(u,v). Our current efforts have resulted in the identification of a very reliable discretized version of the AMPOF. This particular AMPOF's amplitude is ternarized while the phase is binarized. The resulting AMPOF is found to yield much improved statistical performance measures.

Figure 9 shows a gray-level image of a tank. Figure 10a shows the correlation utilizing an undescretized AMPOF while Figure 10b shows the effect having utilized a discretized AMPOF.

In the area of AMPOF based target recognition, we have accomplished the followings:

- Completed testing the viability of the AMPOF in the case of gray-level targets. We have successfully discretized both amplitude and phase of the AMPOF, The discretized AMPOF is being tested currently for both binary and gray-level targets. Such discretization consideration is necessary since AMPOFs will have to be adapted for use with spatial light modulators in an optical set-up. We have also started conducting the minimum average correlation energy (MACE) implementation of the AMPOFs, Our preliminary simulation seems to indicate that the AMPOF-based MACE is better than the, other alternatives
- An optical neural network (NN) implementation of AMPOF based recognition is being studied and simulated to handle scale, rotation, noise, clutter, and obscuration related problems. We do not have significant optical NN-related results at the current time.
- We are currently exploring the use of AMPOF-based MACE for discriminating targets from SAR data,

2.d. ***Neural Networks:*** Neural networks are being investigated for target recognition. Neural networks are characterized by a process of decision making from highly interconnected non-linear thresholding elements known as neurons. Each neuron performs weighted summations on its analog inputs followed by a non-linear, hard limiting threshold function. All these operations are performed in parallel. Software-only neural networks compete heavily for CPU usage and 100% electronic implementations of neural networks are ultimately limited by the massive interconnection requirement between processing elements. We have conducted a literature search to cover the electro-optical implementation of neural networks and the applications that utilized neural networks for target identification or detection.

2.d.1. ***Optical Neural Networks:*** Optical implementations of a neural networks [12,13] are thus motivated by the huge number of interconnections that can be provided by the interferenceless

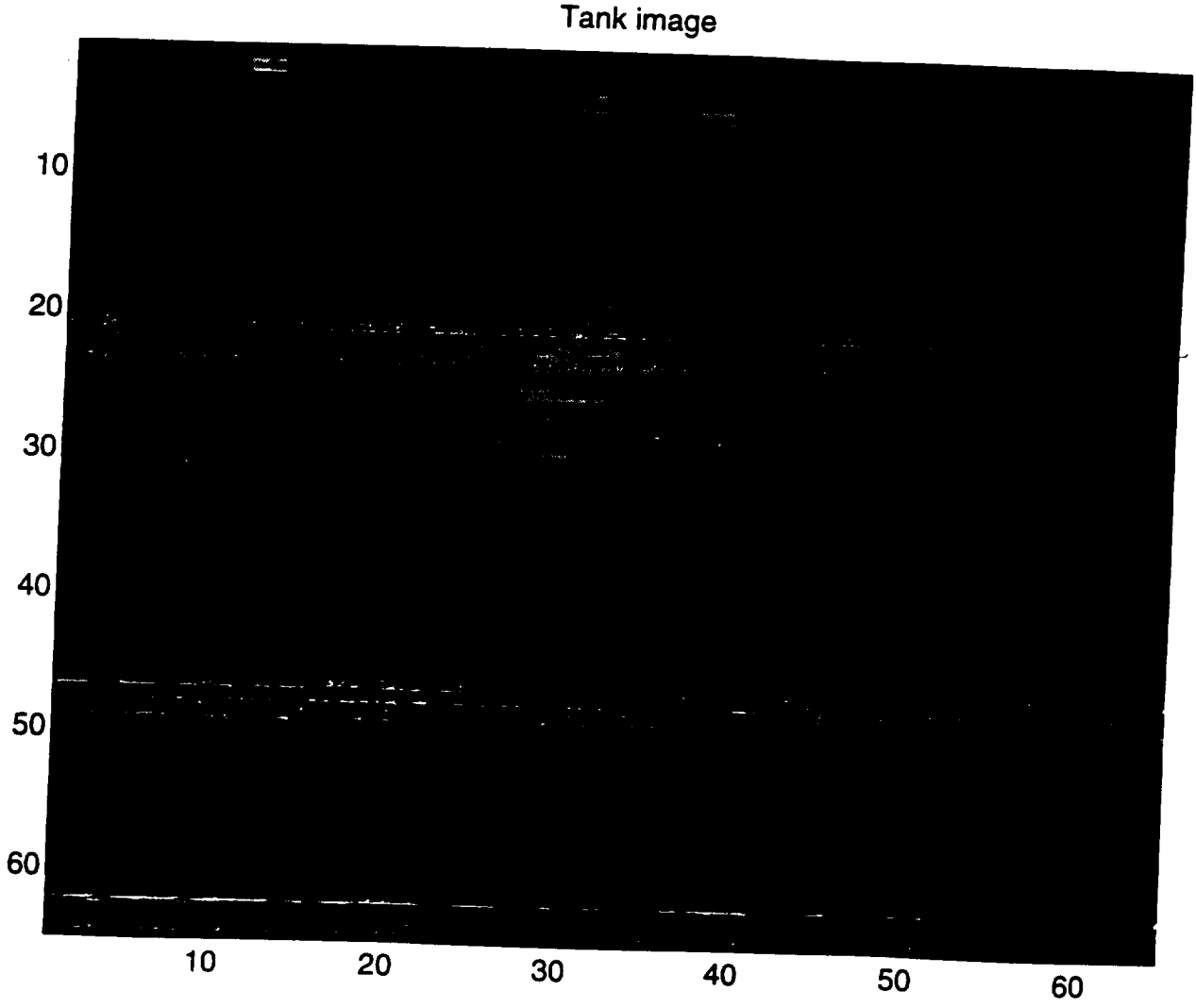

Figure 9, Grey-Level Image of a Tank

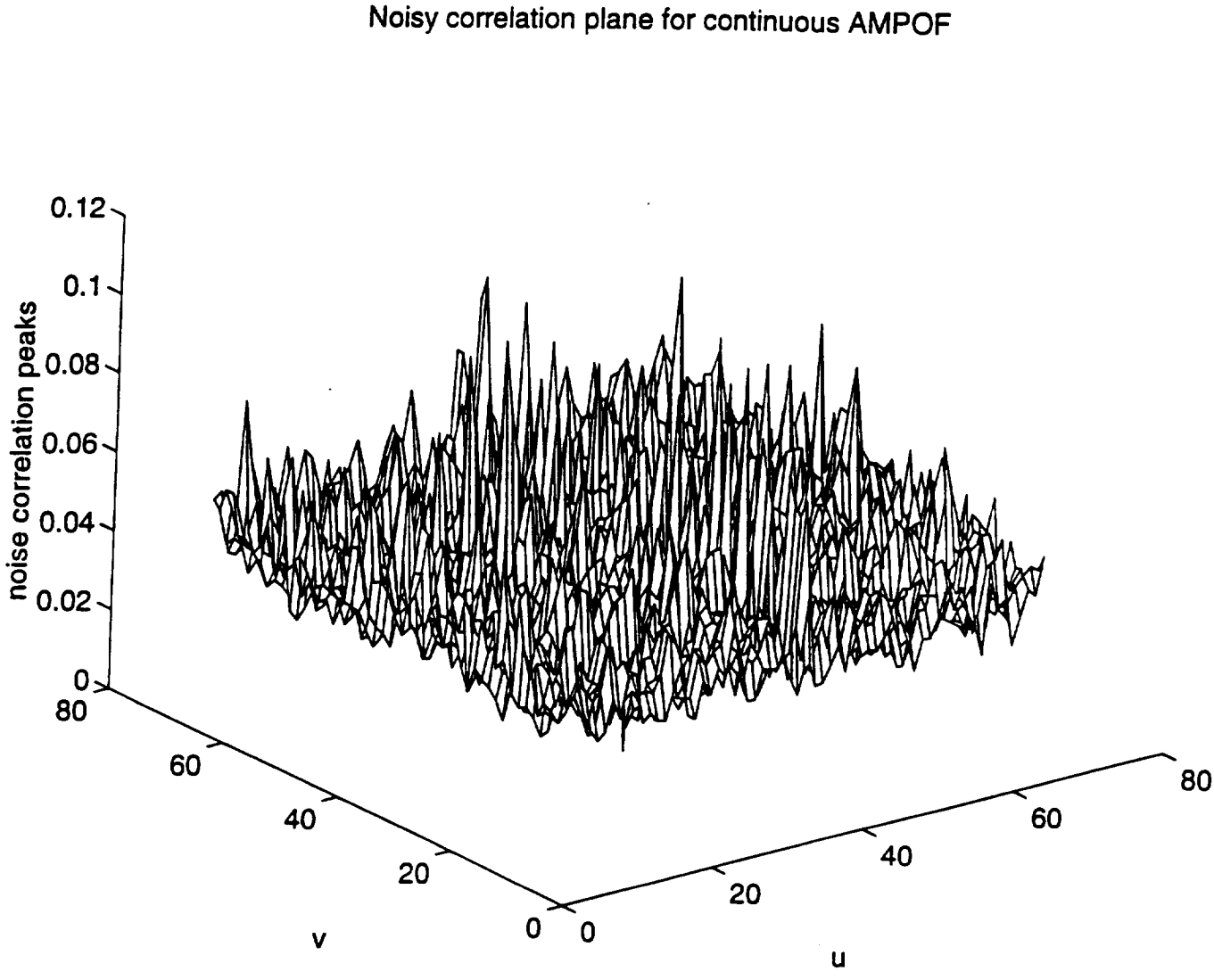

Figure 10a, Correlation Utilizing and Undescretized AMPOF

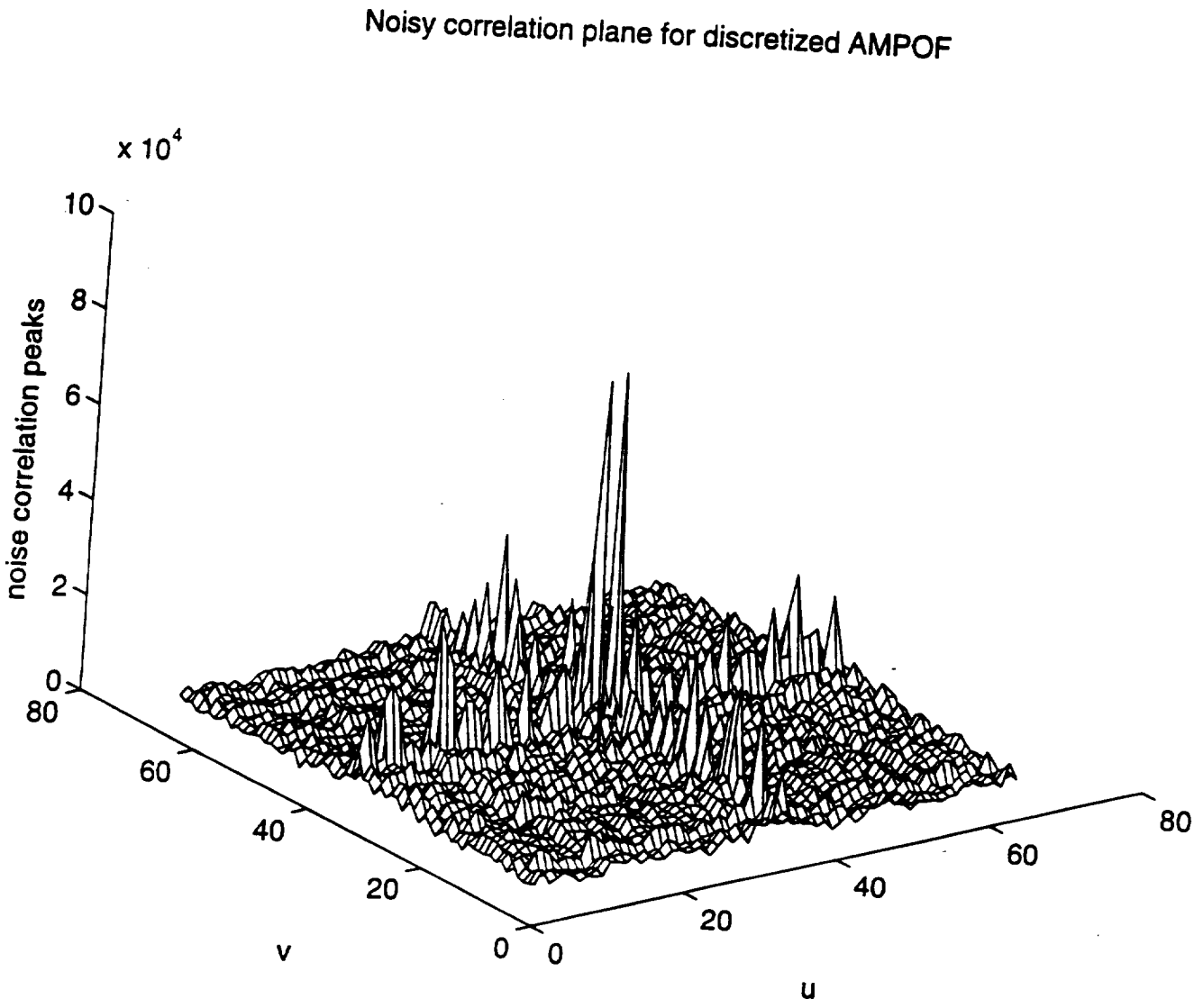

Figure 10b, Correlation Using Discretized AMPOF

free-space parallel communication capabilities of optics. Electro-optics is an efficient and natural way to implement these functions, however, it is not without practical problems. Optical neural processors are usually designed around ultra high speed optical vector-matrix multipliers [14], where the input to the neurons are represented by the vectors while the interconnection weights are represented by the matrix. One of the earliest optical neural network that was implemented was the Hopfield memory [15] model in 1985 by Farhat et al [16]. Many variations of the Hopfield neural networks [17-22] has been proposed and tested for moving target recognition [20], character recognition [21] and machine parts recognition [22]. Additionally, some models of neural networks require training [23]. Training is a process whereby the weight matrix is altered until the output after thresholding, for a given input, conforms to a preselected value. Training is an area where a simple optical implementation may limit a neural network's pattern matching versatility [24]. Clearly, then, many decisions must be made when designing a practical implementation of an electro-optic artificial neural-network. This work provides some basis of how such decisions may be made in the design of an opto-electronic neural network.

Additionally, neural networks are analog circuits. In any analog implementation there are errors associated with the limited analog accuracy and non-linear responses of the components. In electro-optic neural-networks, these errors could exist in the input devices, the interconnection weight matrix , or the output detectors. Neiberg, et. al. have shown that errors in the weight matrix have the most significant impact on the output values [24]. Piche has analyzed weight matrix accuracy and developed methods to quantify the signal to noise ratio of the system based upon these accuracy [25-30] .

2.d.2. ***Neural Network Experiment:*** In target identification, one of the difficult tasks has been the extraction of features to train the neural network which is subsequently used for the target's identification. This section describes the development of an automatic target identification system using features extracted from a specific class of targets. The extracted features were the graphical representations of the silhouettes of the targets. Image processing techniques and some Fast Fourier Transform (FFT) properties were implemented to extract the features. The FFT eliminates variations in the extracted features due to rotation or scaling.. A Neural Network (NN) was trained with the extracted features using the Learning Vector Quantization paradigm. An identification system was set up to test the algorithm. The image processing software was interfaced with MATLAB Neural Network Toolbox via a computer program written in C language to automate the target identification process. The system performed well as it classified the objects used to train it irrespective of rotation, scaling, and translation . This automatic target identification system had a classification success rate of about 95%.

In building a recognition or an identification system using a neural network, a key problem that arises is the extraction of features of the targeted object to be used for training the neural network [31]. The performance of an identification system may be erroneous if the extracted features are subjected to change by factors that were not considered during the training process. If precautions are not taken, factors such as scaling, object rotation, and translation may affect the extracted features and influence the performance of the neural network.

An important problem in pattern analysis or target identification is the automatic identification of a target regardless of its position, size and orientation in a scene [32]. In order to achieve such automation, the feature acquisition tool and the artificial intelligence model (fuzzy logic, neural network, statistical classifiers, etc.) used for identification need to be integrated.

In this study, an algorithm was developed for target identification. The effects of variations due to scaling, rotation, and translation were considered. Neural networks have different paradigms which can be used to develop an identification system. The various paradigms have their pros and cons as far as performance is concerned, depending upon the type of data or features available. For our application, a Learning Vector Quantization (LVQ) network was used. The LVQ is a method for training competitive layers in a supervised manner. The LVQ networks learn to classify input vectors into target classes chosen by the user.

The initial step in the neural network approach for target identification is feature extraction [35-38]. The feature considered in this study was the graphical representation of the silhouette of each target. Five targets were utilized to develop and test the algorithm. Figure 11 shows five aircraft models used in this study. The resources used for developing and implementing the algorithm were: 1) Image processing software package by Epix Inc.; 2) Digital Charge Coupled Device (CCD) black and white video camera; 3) Video monitor; 4) Microsoft *CIC++* software package; 5) MATLAB Neural Networks Toolbox; and 6) 486DX PC. A data flow diagram, shown in Figure 12, depicts how input data (target) is transformed to output results (extracted features) through a sequence of functional transformations.

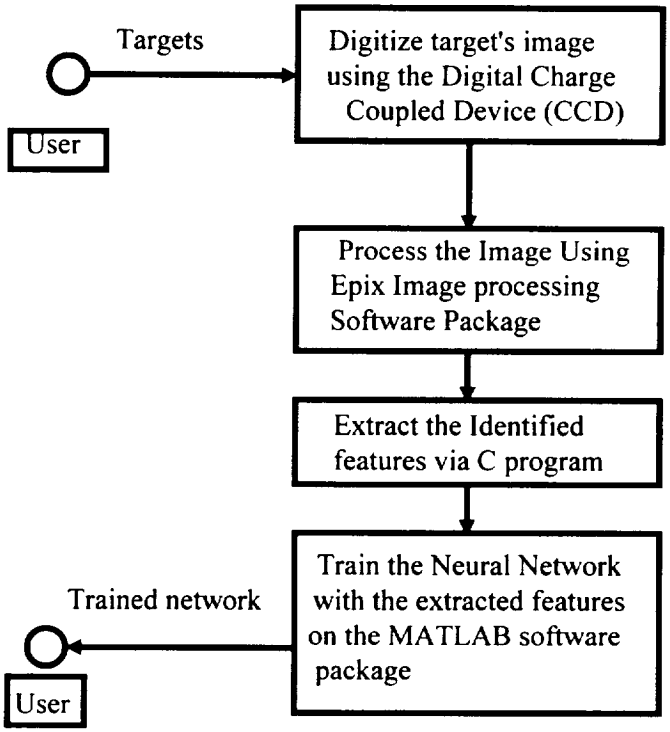

Figure 12 Data flow diagram for feature acquisition and neural network training

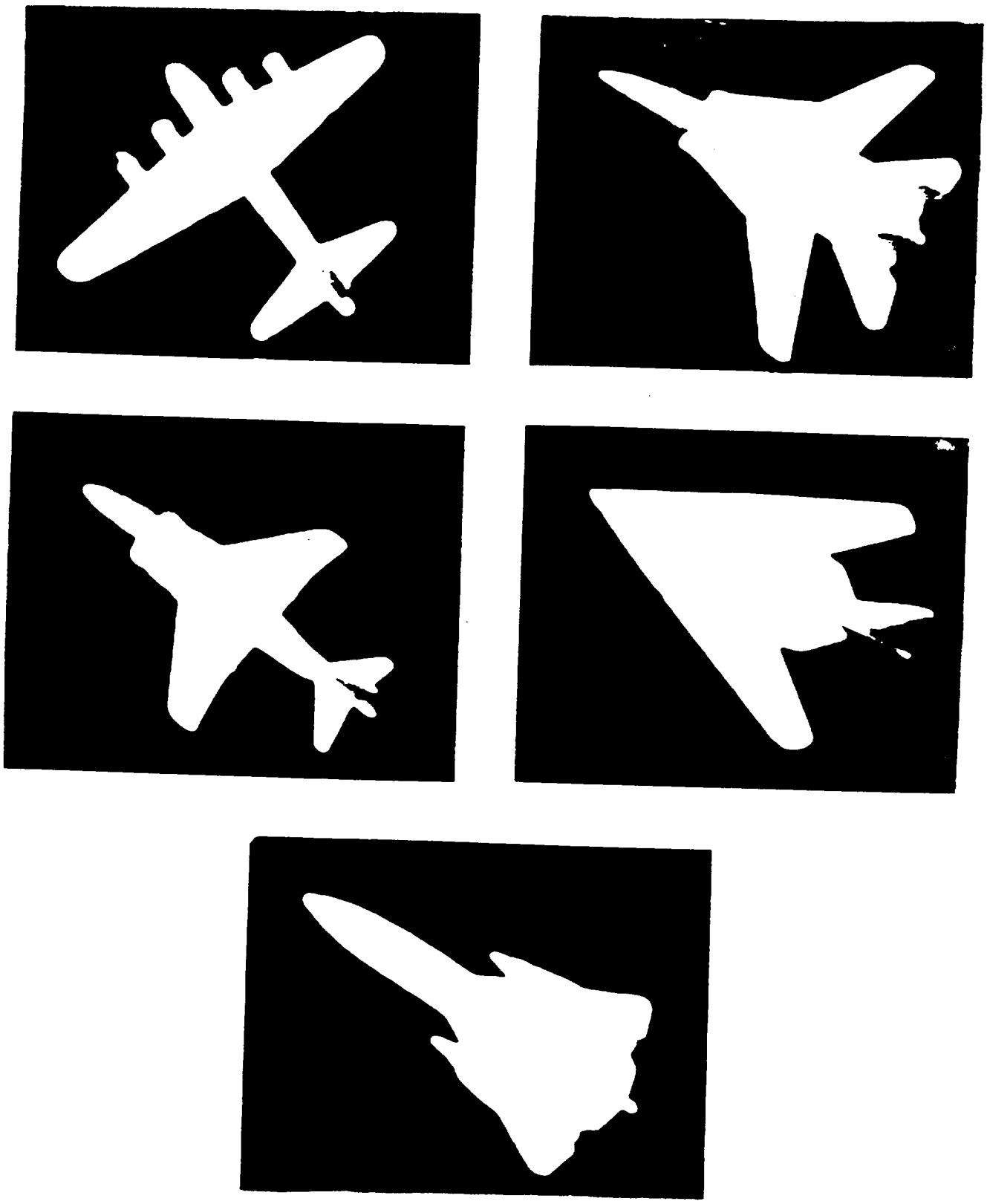

Figure 11, Aircraft Models used in the Study

Live images of the targets (aircraft) were first digitized using the CCD video camera. Using the Epix image processing software package, the images were processed and their boundary outlines (silhouettes) isolated. The centroid of each image was also determined using the Epix software. The silhouettes were thinned to a single boundary line. Figure 13 shows one of the images and its corresponding boundary outline.

A boundary tracking algorithm was developed to transform the silhouette into graphical form. While tracking the boundary, the distance (radius) between each point on the boundary and the centroid was determined. The ratio of each radius to the longest radius was also computed. These radii ratios constituted the variables in the function that represented the silhouette graphically. Figure 14 shows the graphical representation of the boundary function of Figure 13. Using the Fast Fourier Transform, the magnitude of the frequency spectrum was obtained and plotted as shown in Figure 15. It can be seen that the significant amplitudes occur at the two ends of the graph; it is important to note, however, that the first half of the plot along the frequency axis is symmetrical to the other half. As a result, the significant amplitudes of only the first half (100 points) were chosen and utilized as the input or feature for training the neural networks. The plot of the first 100 points in Figure 15 has been expanded and is shown in Figure 16 for elaboration. The same feature was extracted for all targets.

The Neural Network Toolbox in the MATLAB software package was used to train the extracted features. The MATLAB software interfaces with a C program which was developed to access the image processing functions of Epix for extracting the features. The learning paradigm used in this training was the Learning Vector Quantization (LVQ).

Learning Vector Quantization is a method for training competitive layers in a supervised manner. LVQ networks learn to classify input vectors into target classes chosen by the user [34]. The LVQ is composed of two layers: competitive layer and linear layer. The LVQ network is initialized, trained, and simulated with initlvq, trainlvq, and simulvq MATLAB functions respectively. The function initlvq initializes the weights W1 and W2 for the competitive and linear layers respectively. The function trainlvq is used to train the network. The training uses the initialized weights, W1 and W2, the input signal (extracted feature) and the target (class) vectors, and the parameters for the learning function. The class indices are converted to vectors with IND2VEC function to obtain the network's target vectors.

The maximum number of epochs was 1000 and the learning rate was 2. Only one output neuron of the linear layer would have an output of 1 depending upon the class of the input vector during and after training. The rest of the output neurons would have Os.

The function simulvq was used to test the trained network. Simulvq takes the saved weights, and an input vector, and returns the class for that particular vector. A series of experiments was performed to test the effectiveness of the algorithm developed in this study. The main theme of this algorithm was to use the properties of Fast Fourier Transform to eliminate the effect of any variation in the extracted features and use the extracted features for target identification. The five

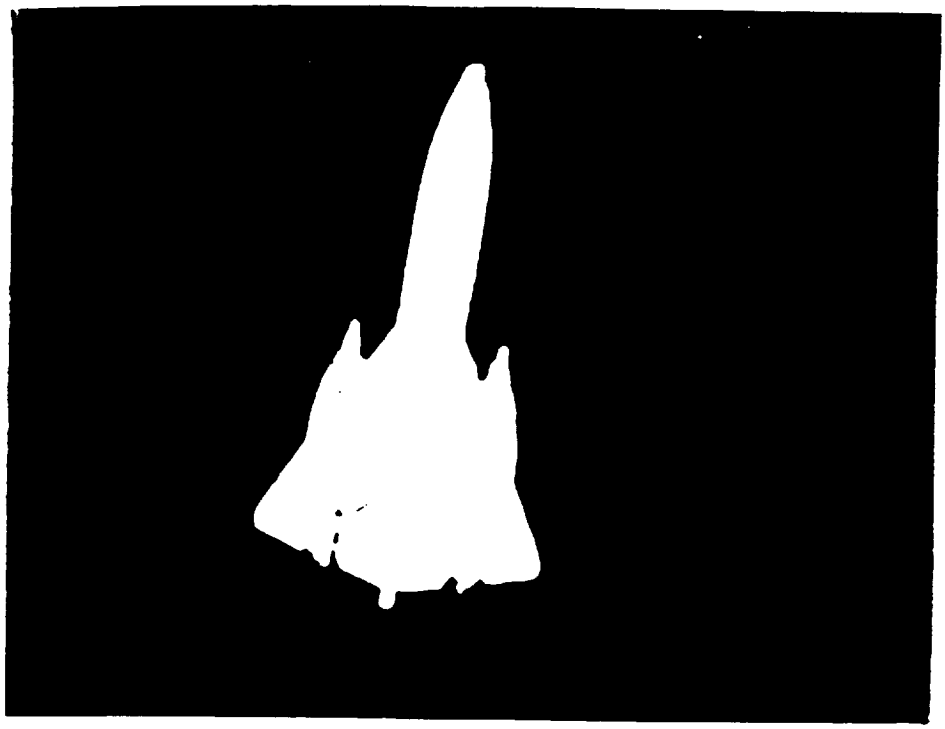

Figure 13, One of the Aircrafts

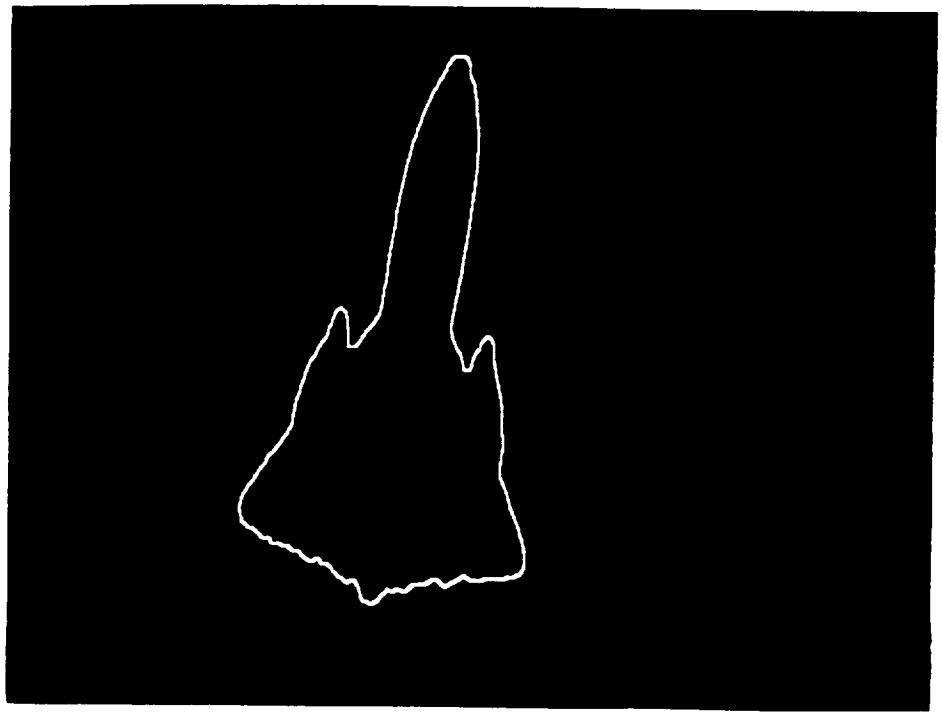

Figure 14, Corresponding Silhouette

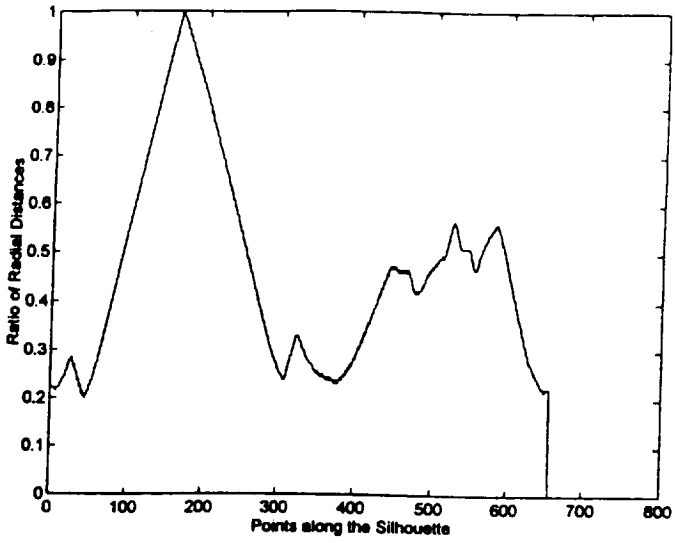

Figure 15, Silhouette Function

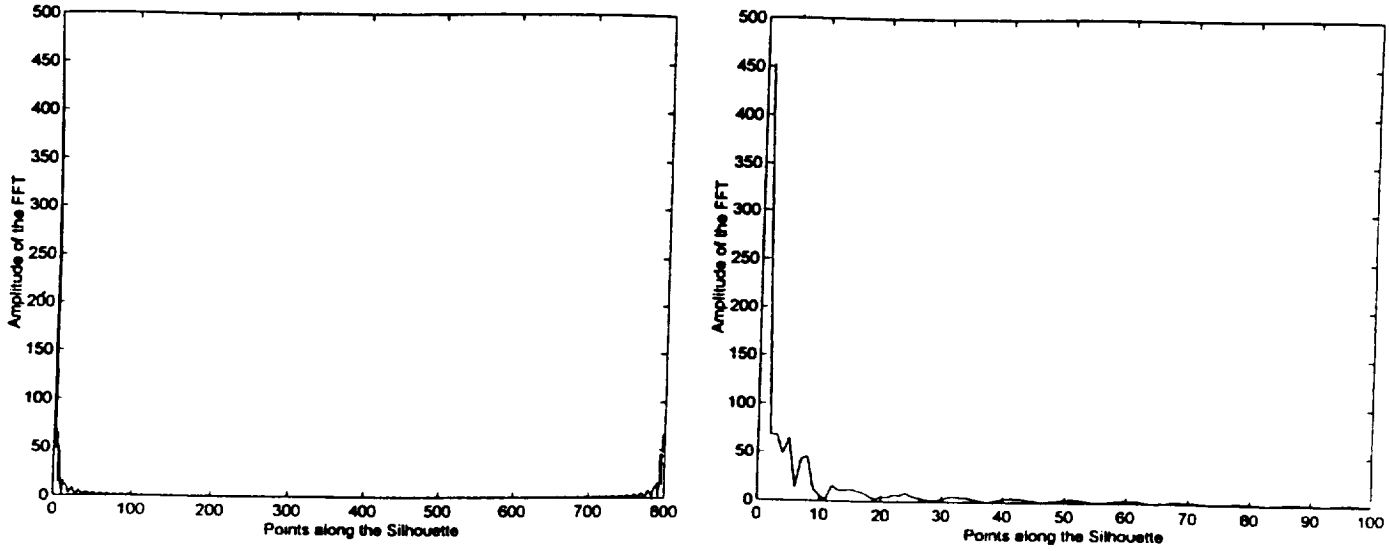

Figure 16, FFT of the Silhouette Function

aircraft in Figure 11 were used to test the algorithm. For each aircraft, various possible conditions were tested. Each aircraft was translated, rotated at different angles, reduced to about 50% in area, and both increased about 100% in area and rotated at different angles. Figure 17 shows the images of the five aircraft in their respective conditions under which the experiment was conducted. The normal condition is the initial condition under which the features used in training the neural network were extracted.

The classification accuracy is summarized in Table 1. The number of misclassifications represents the number of times the system misclassified any of the targets under the stated conditions. For each condition about fifty trials were made. For example. the '5' in the number misclassified column represents five misclassification in fifty trials when the targets were both scaled 100% in area and rotated at different angles. The results obtained show the reliability and the high accuracy of this algorithm. Each classification or trail was performed in twelve seconds or less. However, this time could be significantly reduced by replacing the 50 MHz 486 PC with a Pentium or higher performance workstation.

Condition	Number Misclassified	Percent Correct
Normal	0	100%
Rotated at different angles	0	100%
Translated	0	100%
Reduced to about 50% in area	0	100%
Increased to about 100% in area and rotated	5	90%

Table 1 Classification Results

2.e. ***Model based target Recognition:*** Previously, we utilized neural network to classify target using their silhouettes. Additionally, a bivariate autoregressive model [39] is utilized for the analysis and classification of closed planar shapes. The boundary coordinate sequence of a digitized binary image is sampled to produce a polygonal approximation to an object's shape. This circular sample sequence is then represented by a vector autoregressive difference equation which models the individual Cartesian coordinate sequences as well as coordinate interdependencies. Several classification features which are functions or transformations of the estimated coefficient matrices and the associated residual error covariance matrices are exploited. These features are shown to be invariant to object transformations such as translation, rotation and scaling. Laboratory experiments involving an object set representative of military aircraft is presented.

Here, we present preliminary results for our work in target boundary analysis and classification. We explored a scalar transform technique which is an extension of the methods based on one-dimensional (1-D) Circular Autoregressive (CAR) models [40,41]. A given target silhouette is approximated by N samples of its original boundary sequence. The x and y Cartesian coordinates of these samples referenced to the object centroid serve as the elements of a bivariate spatial series. This bivariate series is then represented by a stochastic circular autoregressive model characterized by a set of unknown coefficient matrices and an independent vector noise

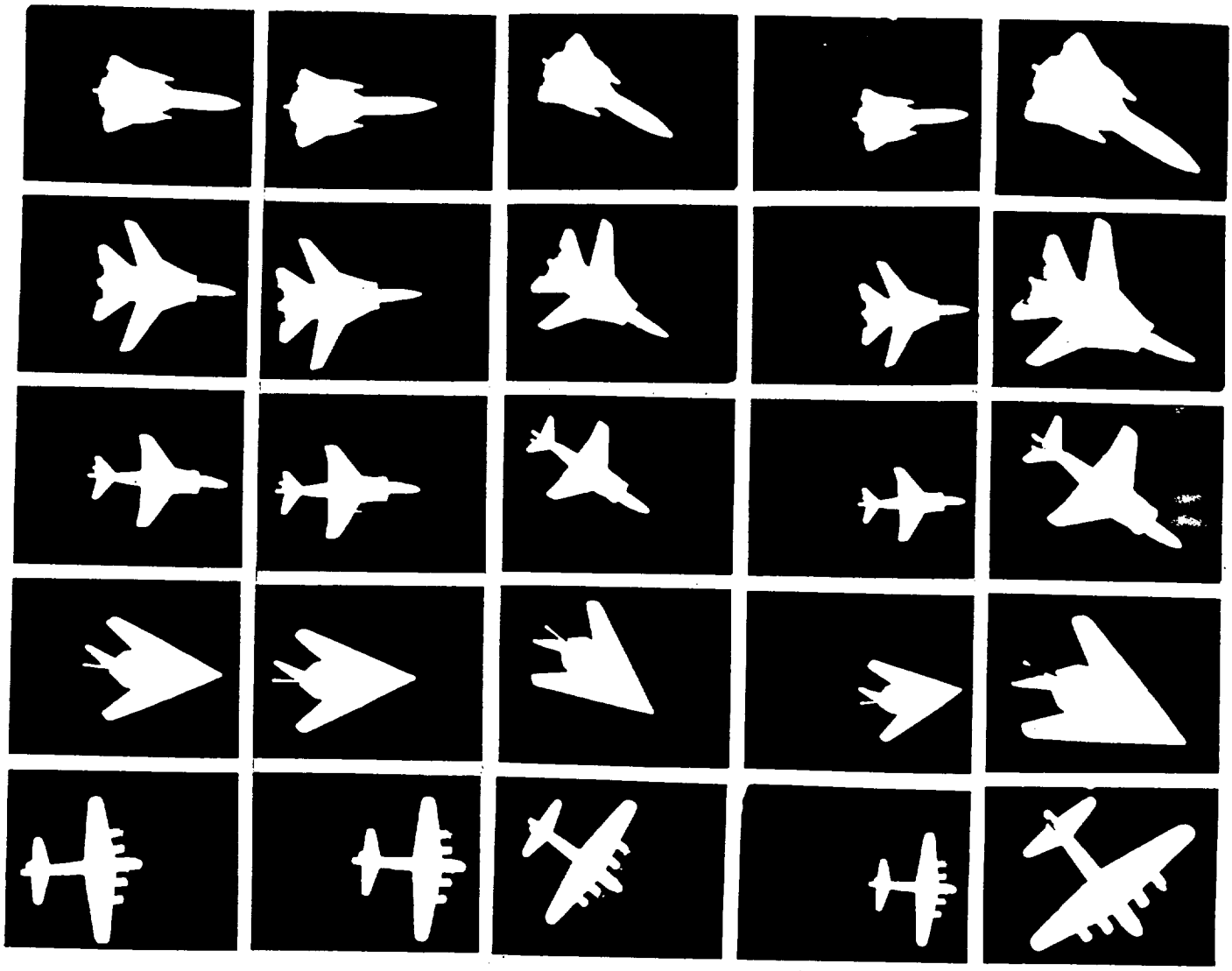

Figure 17. Test Aircraft Models

sequence. Certain functions of these matrices are introduced and shown to be invariant to rotation, translation, and scaling.

A bivariate sequence representation has certain advantages over one dimensional methods. Since both the x and y coordinates of the shape boundary are used, both convex and non-convex objects may be treated in the same fashion. Although boundary unwrapping techniques [40] allow the extension of radii based methods to non-convex shapes, they lose boundary phase information. Such phase loss can allow different shapes to produce similar sequences. A bivariate boundary representation allows a variety of sampling schemes to be used. Because of this flexibility it is sometimes possible, depending upon the data set, to choose a sampling method which biases the resulting spatial series so as to improve classification results. A presentation on the issues involved in the choice of sampling rate and method for shape analysis can be found in [42]. Finally, the bivariate method allows the modeling of the x and y coordinate sequences as well as the inter-relationships between them. We have found that this results in models with lower residual errors than that achieved with a one dimensional model. Also, extension of this bivariate method to sequences described on higher dimensional lattices is straightforward. Other two-dimensional methods which provide context for our algorithm can be found in [40,43,44].

Since the shape boundaries are closed contours, we have X(i) = X(i+N), where {X(i), i=1,2,...N) are coordinates of the boundary samples used to approximate the shape. We choose to fit the following circular autoregressive model:

$$Y(k)=\sum_{j=1}^{p} A_j Y(k-j)+ \sqrt{\beta}\, VY(k), \qquad k=1,2,...,N$$

$$X(k)=\alpha + Y(k)$$

where $\{A_j, j = 1,2,..p\}$ are 2 x 2 coefficient matrices, and α is a 2 x 1 process mean vector, i.e., $E[X(k)] = \alpha$, where E[] denotes the expected value of []· The modeling error is represented by $\sqrt{\beta}\, V(k)$ and is taken as a zero-mean white noise random vector sequence with β as the covariance matrix.

This model may also be written in state space form as follows: Define the following matrices,

$$Y^t(k)= [Y^t(k), Y^t(k-1), Y^t(k-2), ..., Y^t(k-p+1)]^t,$$

$$A_s= \begin{vmatrix} A_1 & A_2 & \dots & A_{p-1} & A_p \\ I_2 & 0 & \dots & 0 & A_p \\ 0 & I_2 & 0 \dots & 0 & 0 \\ 0 & 0 & I_2 \ 0 \dots & 0 & 0 \\ 0 & 0 & 0 \dots & I_2 & 0 \end{vmatrix}$$

$X_s(k)= [X^t(k), X^t(k-1), X^t(k-2), ..., X^t(k-p-1)]^t$, $\alpha_s = [\alpha^t, \alpha^t, ... \alpha^t]^t$,

$V_s(k)=[V^t(k) \sqrt{\beta^t}, 0, \cdots, 0]^t$,

then we have, $Y_s(k) = A_s Y_s(K - 1) + V_s(k)$, $X_s(k) = \alpha_s + Y_s(k)$,

where A_s is the 2p x 2p system matrix, and I_2 is a 2 x 2 Unit matrix.
In order for this model to be useful for shape classification, features which are invariant to changes in shape rotation, scaling, and translation must be identified. We may state the following Theorem:

Theorem 1: Consider a circular vector sequence {X(i), i=1,2,...N}, whose elements are boundary sample coordinates (referenced to an objects centroid) from a simply connected closed planar shape curve. If the sequence is modeled by the vector circular autoregressive model (CAR) given in (1) and (2), then the following features are invariant to translation, arbitrary rotation, and scaling of the shape:

(a) the trace, determinant, eigenvalues, and elemental sum of squares of the coefficient matrices $\{A_j, j=1,2,...p\}$,

(b) the trace, determinant and eigenvalues of the system matrix A_s,
(c) the combination of the mean vector α and the covariance matrix β designated as tau:
$\tau = \alpha^t \beta^{-1} \alpha$ Proof: [39]

The intraclass invariant properties of the system matrix eigenvalues, the sum of squares of the elements of the coefficient matrices, and the mean vector error covariance matrix product, τ make them excellent candidates as target features for recognition purposes. Digitization errors, imaging noise, and parameter estimation errors are among the influences which can cause the feature vectors within the same class to exhibit some variations. These variations will typically generate close clusters in the feature space which can be adequately characterized by a variety of statistical pattern recognition techniques.

2.e.1. ***Experiments and Results:*** The experiments are principally concerned with nonoverlapping simply connected planar shapes which are completely known, i.e., no partial boundaries are considered. The shapes used for the experimental portion of this report are illustrated in Figure 18, and consist of fourteen different aircraft silhouettes some of which are very similar. These shapes, though not extracted from actual imagery, provide a complex set with subtle differences.

Forty images were taken for each plane in the set. The shapes were rotated by arbitrary angles, shifted within the image plane, and scaled by as much as 200 percent by changing the camera magnification. The boundary sequences were obtained by a boundary follower algorithm.

In order to insure the accuracy of the image sample locations and eliminate perimeter dependence in the sampling algorithms, a polygonal approximation was first calculated for each

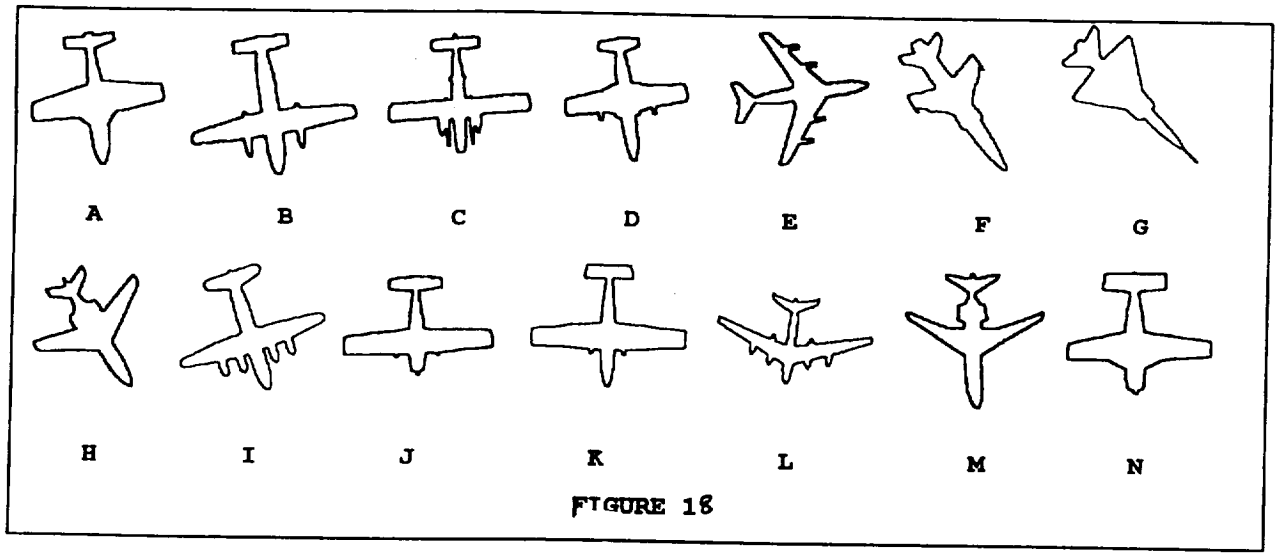

FIGURE 16

shape [45]. The number of polygonal segments for each shape varied depending on the amount of curvature present. The linear segments were fit such that the maximum distance of any boundary point from the corresponding line segment was 2.0 grid units. The resulting polygon was used to determine sample coordinates for the bivariate model. It was found that using samples calculated from the polygonal approximation rather than points taken directly from the boundary sequence resulted in lower overall variance in the feature vectors. The boundary sampling method used to generate the bivariate model sequences was an equal-curve-length method [42] which chooses samples such that they are spaced at equal distances along the shape contour. The sample rate was determined by performing a Fourier power spectral analysis of the most complex shape contours. A rate of 128 samples per object was deemed sufficient to represent the salient boundary variations.

2.e.2 ***Classification Feature Vector:*** The next task is to identify functions or transformations which extract salient information from these matrices while remaining invariant to scaling and rotation. The state space formulation for the CAR model is attractive because the eigenvalues of the system matrix completely identify the system modes, and therefore are excellent feature candidates. Although the eigenvalues of the individual coefficient matrices could also be used as invariant features, they are not capable of completely describing the system modes. However, if a real feature vector is desired, the trace and determinant of the individual matrices can be used effectively as features.

The sum of squares of the elements of the coefficient matrices is used as a feature because it exploits the fact that object rotation results in a unitary transformation rather than just a similarity transformation. A conventional similarity transformation would result in invariant eigenvalues corresponding to an equivalent system, but the sum of squares feature would vary.

The feature τ (see Theorem 1), is important in that it is based on the process mean vector and on the model residual error which is an indication of model fit. An alternative way to incorporate the information in the residual error covariance matrix into the feature vector is to use the

eigenvalues of the quantity $P/(\alpha^t \alpha)$ as features. This allows more detailed information about the quality of the CAR model fit to be used for classification at the cost of increasing the dimension of the feature vector by one. These eigenvalues can be shown to be invariant by following a procedure similar to that presented in the proof of Theorem 1. The actual feature vector used for this study can be written as $[\text{eig}(\hat{A_s}), S(\hat{A_s}), \hat{\tau}]$ where $\text{eig}(\hat{A_s})$ denotes the eigenvalues of the estimated system matrix, and the sum of the squares of the elements of the model coefficient matrices is,

$$S(\hat{A_s}) = \sum_{k=1}^{p} \sum_{i=1}^{2} \sum_{j=1}^{2} (\hat{\alpha_{kij}})(\hat{\alpha_{kij}})^t$$

2.e.3 ***Classification Results:*** A straightforward weighted Euclidean distance classifier (the Feature Weighting method [81) was used to evaluate the quality of the features derived from the bivariate CAR model. The classification results for this study are presented in Table II below. Included in the table are the classification accuracy as well as the 95% confidence interval specified in terms of a classification accuracy window. The limits are calculated using the following equation,

$$\Pr\left\{ \frac{2n\hat{p} + z^2 - z\sqrt{4n\hat{p} + z^2 - 4n\hat{p}^2}}{2(n+z^2)} < p < \frac{2n\hat{p} + z^2 + z\sqrt{4n\hat{p} + z^2 - 4n\hat{p}^2}}{2(n+z^2)} \right\} \cong \psi,$$

where z=1.960, ψ=0.95, n is the total number of test samples, and $\hat{p}$ is the maximum likelihood estimate for the error rate = (#misclassifications)/n.

Table II
Bivariate CAR Model Classification Results

order 1	
Misclassifications	0
Percent correct	100
95% Confidence Interval	98.65 ⇔ 100
order 2	
Misclassifications	0
Percent correct	100
95% Confidence Interval	98.65 ⇔ 100

3- Conclusions

In this report we investigated a promising approaches for the automated target recognition and identification. Electro-optic techniques provides high speed processing as two dimensional image processing is accomplished in parallel. Neural networks were utilized and proved effective in target identification using images of target aircrafts under different conditions. Another approach for generation of salient classification features from a target's boundary contour was developed. A bivariate circular autoregressive model of a sampled shape's boundary sequence was used to develop a set of classification features which were shown to be invariant to object translation, rotation, and scaling. Laboratory experiments demonstrated superior classification accuracy (100%) at low model orders. These boundary features then, are likely candidates for use in conjunction with other topological and structural features in a general automatic target recognition system. Further testing with actual imagery will be necessary to determine the model's efficacy in more realistic environments.

4- Publications

[1] Mahmoud A. Abdallah, Tayib I. Samu, and William A. Grissom, "Automated Target Identification Using Neural Networks," SPIE's Photonics East Symposium, 22-26 October 1995, Philadelphia, Pa.

[2] Farid Ahmed and Mohammad A. Karim, "Filter-Feature-Based rotation-invariant Joint Fourier Transform Correlator," Applied Optics, Vol. 34, No. 32, pp. 7556-7560, November 1995.

[3] Farid Ahmed, M.A. Karim, and M.S. Alam, "Wavelet Transform-Based Correlator for the Recognition of Rotationally Distorted Images," Optical Engineering, Vol. 34, No. 11, pp. 3187-3192, November 1995.

5- References

[1] M. A. Karim, *Electro-Optical Devices & Systems*, PWS-Kent Pub., Boston, Mass, 1990.

[2] M. A. Karim, and A. A. S. Awwal, *Optical Computing: An Introduction*, John Wiley, New York, NY, 1992.

[3] D. Casasent, and D. Psaltis, "New Optical Transforms for Pattern Recognition," *Proc. IEEE.*, Vol. 65, pp. 77-84, 1977.

[4] D. Casasent, and D. Psaltis, "Position, Rotation, and Scale Invariant Optical Correlation," *Applied Optics*, Vol. 15, pp. 1795-1799, 1976.

[5] B. Javidi, and C. Kuo, "Joint Transform Correlation Using a Binary Spatial Light Modulator at the Fourier Plane," *Applied Optics*, Vol. 27, pp. 663-665, 1988.

[6] 0. Perez, and M. A. Karim, "An Efficient Implementation of Joint Fourier Transform Correlation Using a Modified LCTV," *Microwave Opt. Technol. Lett.*, Vol. 2, pp. 193-196, 1989.

[7] M. S. Alam, and M. A. Karim, "Fringe-Adjusted Joint Transform Correlation," *Applied Optics*, Vol. 32, pp. 4344-4350, 1993.

[8] M. S. Alam, and M. A. Karim, "Joint Transform Correlation Under Varying Illumination," *Applied Optics*, Vol. 32, pp. 4351-4356, 1993.

[9] J. L. Horner, and P. D. Gianino, "Phase-Only Matched Filtering," *Applied Optics*, Vol. 23, pp. 812-816, 1984.

[10] A. A, S. Awwal, M. A. Karim, and S. R. Jahan, "improved Correlation Discrimination Using an Amplitude Modulated Phase-Only Filter, " *Applied Optics*, Vol. 29, pp. 233-237, 1990.

[11] S. H. Zheng, M. A. Karim, and M. L. Gao, "Amplitude-Modulated Phase-Only Filter Performance in Presence of Noise, " *Opt, Commun.*, Vol. 89, pp. 296-305, 1992.

[12] *Applied Optics,* Special issue on Optical neural Network, 10 March 1993

[13] J. W. Goodman, A. R. Dias, and L. M. Woody, "Fully parallel high speed incoherent Optical Method for performing discrete Fourier Transforms," *Opt. Lett.,* Vol. 2, pp. 1-3, (1978).

[14] J. J. Hopfield, "Neural networks and physical systems with emergent collective computational abilities," *Proc. Natl. Acd Sci.,* USA, Vol. 79, pp. 2554-2558, (1982).

[15] N. Farhat, D. Psaltis, A. Prate, and E. Paek, "Optical implementation of the Hopfield model,", *Applied Optics,* Vol. 24, pp. 1469-1475 (1985)

[16] R. J. Marks, "Class of continuous level associative memory neural nets," *Applied Optics* Vol. 26, pp. 2005-2010 (1987)

[17] D. Feng, H. Chen, S. Xia and K. Xu, "Optical bipolar k^{th}-order neural network based on inner-product representation," *Applied. Optics,* Vol. 33, pp. 6235-6238, (1994)

[18] C. H. Wu and H. K. Liu, "Unipolar terminal-attractor-based neural associative memory with adaptive threshold and perfect convergence," *Applied. Optics.,* Vol. 33, pp. 2210 -2217, (1994)

[19] A. A. S. Awwal and G. Power, "Object tracking by an opto-electronic inner product complex neural network, *Opt. Engg.*, Vol. 32, pp. 2782-2787, 1993.

[20] F. Ahmed and A. A. S. Awwal, "An adaptive opto-electronic neural network for associative Pattern Retrieval," *J. of parallel and distributed comp.*, Vol. 17, pp. 245-250, 1993.

[21] A. A. S. Awwal , M. A. Karim and H. K. Liu, "Machine Parts Recognition using a Trinary Associative Memory," *Applied. Optics* ,Vol. 28, pp. 537-543, 1989.

[22] A. D. Fisher, W. L. Lippincott, and J. N. Lee, "Optical implementations of associative networks with versatile adaptive learning capabilities," *Applied Optics,* Vol. 26, pp. 5039-5054 (1987)

[23] L. Neiberg and D. Casasent, "High-Capacity Neural Networks on Non ideal Hardware," *Applied Optics,* Vol. 33, no. 32, pp. 7665-7675 (1994)

[24] S. W. Piche, "The Selection of Weight Accuracies for Madalines," *IEEE Transactions on Neural Networks,* Vol. 6, no. 2, pp. 432445 (1995)

[25] R. C. Frye, E. A. Reitmann, and C. C. Wong, "Backpropagation Learning and Non idealities in Analog Neural Network Hardware," *IEEE Transactions on Neural Networks,* Vol. 2, pp. 110-117(1991)

[26] S. P. Luttrell, "Derivation of a Class of Training Algorithms," *IEEE Transactions on Neural Networks,* Vol. 1, pp. 229-232 (1990)

[27] W. Belter, M. Takahashi, J. Ohta, and K. Kyuma, "Weight quantization in Boltzmann machines," *Neural Net.*, Vol. 4, pp. 405-409 (1991)

[28] M. Hoefeld and S. Faflman, "Learning with limited precision using cascade correlation algorithm," *IEEE Transactions on Neural Networks,* Vol.3, pp. 602-611 (1992)

[29] W. Robinson, *Character Recognition Using Novel Optoelectronic Neural Network,* MS Thesis, University of Texas at San Antonio (1993)

[30] R. P. Webb, "Performance of an optoelectronic neural network in the presence of noise," *Applied Optics,* Vol. 34, no. 23, pp. 5230-5240 (1995)

[31] Gilmore. J. F, and Czuchry, A. J. Jr., "Target detection in a neural network environment," *SPIE* Vol. 1293 Applications of Artificial Intelligence VIII (1990), pp. 301-317.

[32] Imai, Gouhara K, and Uchikawa, Y., "Pattern extraction and recognition for noisy images using the three-layered BP model," *IEEE 91*, pp. 262-267.

[33] Khotanzad, A. and Hong Y. H. "Invariant image recognition by Zernike moments." *IEEE transactions on pattern analysis and machine intelligence*, Vol. 12, No. 5, pp. 489-497. May, 1995.

[34] Demuth, D, and Beale M., *Neural Network Toolbox,* The Math Works Inc.: Natick. 1994

[35] Sun, Y. "Neural network approach for classification using features extracted by mapping." *Pattern Recognition letters* 14. pp. 749-752, 1993.

[36] Grace, A. E and M. Spann. "A comparison between Fourier-Mellin descriptor and moment based features for invariant object recognition using neural networks." *Pattern Recognition Letter*, 12, pp. 635-643, 1991.

[37] Gupta, L., M. R. Sayeh and R. Tammana. "A neural network approach to robust shape classification," *Pattern Recognition*, 23 (6), pp. 563-568, 1990.

[38] Khotanzad, A. and J. Lu. "Classification of invariant image representations using a neural network," *IEEE trans. Acoust. Speech Signal Process*, pp. 38-44, 1990.

[39] M. Das, M. J. Paulik, and N. K. Loh, "A Bivariate Autoregressive Modeling Technique for Analysis and Classification of Planar Shapes," *IEEE Trans. Pattern Anal. Mach. Intell.*, Vol. PAMI-12, No. 1, pp. 97-103, Jan. 1990.

[40] R. L. Kashyap and R. Chellappa, "Stochastic models for closed boundary analysis: Representation and reconstruction," *IEEE Trans. Inform. Theory,* Vol. IT-27, No. 5, pp. 627-637, Sept. 1981.

[41] S. R. Dubois and F. H. Giant, "An autoregressive model approach to two dimensional shape classification, " *IEEE Trans. Pa t tern Anal. Mach. Intell.*, Vol. PAMI-8, No. 1, pp. 55-66, Jan. 1986.

[42] M. J. Paulik, *Analysis and Classification of Planar Shapes and Textures Using Stationary and Spatially Varying Autoregressive Models.* Ph.D. Dissertation, pp. 62-77, Oakland University, Rochester MI, 1989.

[43] C. C. Lin and R. Chellappa, "Classification of partial 2-D shapes using Fourier descriptors," *IEEE Trans. Pattern Anal. Mach. Intell.*, Vol. PAMI-9, No. 5, pp. 686-690, Sept. 1987.

[44] E. Persoon and K. S. Fu, "Shape discrimination using Fourier descriptors," *IEEE Trans. Syst., Man, Cybern.*, Vol., SMC-7, No. 3, pp. 170-179, Mar. 1977.

[45] T. Pavlidis, *Algorithms for Graphics and Image Processing.* Maryland: Computer Science Press, *1987.*

[46] G. S. Sebestyen, *Decision-Making Processes in Pattern Recognition.* New York: Macmillan; 1962.

6- ATTACHMENTS

Financial Report

7- DISTRIBUTION

Mr. Steve Sawtelle, WL
Mr. Robert Tegtman, OAI
Dr. Moahmmad Karim, UD
Dr. Nizar Al-Holou, UDM
Dr. A. A. S. Awwal, WSU